12. Conclusions

The objective of this work is, as stated in Chapter 1, to characterize the CO oxidation reaction over gold with all relevant adsorbate-substrate binding energies and reaction activation energies, supplemented with information about the electronic and geometric structure of the adsorbate phases. The results reported in Chapters 5-11 now enable us to quantify the schematic energy diagram in Fig. 1.1 with the respective energy values determined for our system. This quantified diagram is displayed in Fig. 12.1.

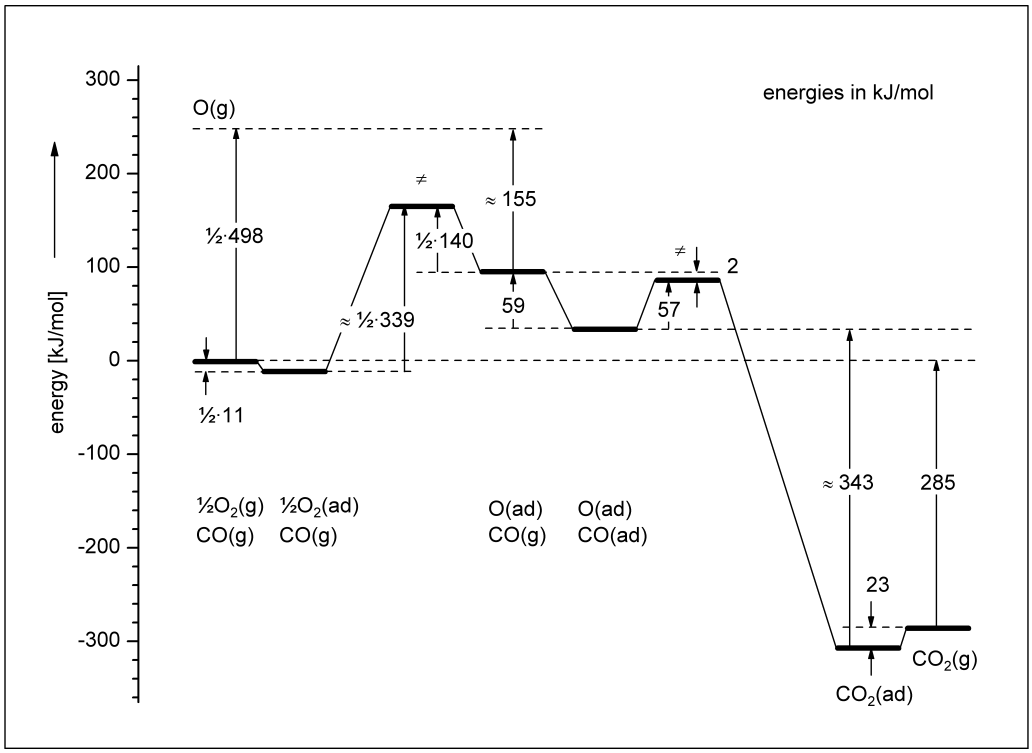

Fig. 12.1: Quantitative energy diagram of the CO oxidation over Au(110)-(1×2). All values concerning dioxygen adsorption are multiplied with 1/2 to account for the stoichiometry of the reaction which requires only 1/2 O_2 for the oxidation of one CO molecule. All values (apart from the standard gas phase reaction energy of 285 kJ/mol and the O_2 dissociation energy of 498 kJ/mol) were taken from Chapters 5-11.

We start on the left hand side of the diagram. The only spontaneous interaction of the (ground-state) oxygen molecule with a Au(110)-(1×2) surface is physisorption with an O_2-Au binding energy of less than 12 kJ/mol. Accordingly, O_2 adsorbs in UHV only below 50 K. In a thermal desorption experiment, we observe three first-order desorption states at 51 K and 45 K (first layer), and at 37 K (second layer). The monolayer coverage corresponds to 0.51×10^{19} oxygen molecules per m^2, which is equivalent to 1.2 O_2 molecules per surface unit cell (2.89 Å × 8.16 Å). Low-energy electron diffraction does not reveal any ordered adsorbate structure, nor does an angle-resolved UV photoemission

experiment reveal any dispersion. Both UPS and NEXAFS spectra indicate mere physisorption of the oxygen molecules on the gold surface.

The dissociative chemisorption of O_2 on our gold surface is obviously highly activated, since neither a chemisorptive nor dissociative adsorption of dioxygen was observed in the temperature range 30-700 K, nor was a spontaneous conversion of the physisorbed into chemisorbed oxygen (as it was found on silver surfaces) observed. To the best of our knowledge, this inertness towards molecular oxygen distinguishes the gold surface from all other metal surfaces investigated hitherto and allows the study of unperturbed oxygen physisorption. The data presented in Chapters 6 and 7 provide an estimated value of 339 kJ/mol for the activation energy for dissociative chemisorption (a value which is still substantially lower than the gas phase dissociation energy of 498 kJ/mol). In light of the heterogeneously catalysed CO oxidation, we can conclude that the crucial step of this reaction, the spontaneous cleavage of the O-O bond, cannot occur on a Au(110)-(1×2) surface and, probably, generally not on extended gold samples. Thus, the ability of the real catalysts (which consist of oxide-supported gold clusters) to cleave O_2 is connected with the size of the clusters or with a promotive effect exerted by the oxidic support. In fact, many authors have concluded on the basis of sound evidence that the reaction site is located at the junction between gold cluster and support. This idea is confirmed by the observation that large supported and unsupported gold particles are inactive, whereas active catalysts can be made by depositing titania (TiO_2) onto gold powder, or gold onto a titania single crystal (see [Bo00] for references).

In order to generate chemisorbed oxygen phases for further studies of the CO oxidation, we employed two somewhat complementary methods for producing chemisorbed oxygen phases, namely, electron bombardment of physisorbed O_2 and ion bombardment with O^+/O_2^+. We had observed that electron bombardment of physisorbed or condensed oxygen adlayers induces chemical reactions within these adlayers, resulting in the formation of chemisorbed oxygen on the gold surface (UV irradiation has a similar effect). Since the amount of chemisorbed oxygen depends on easily controllable parameters such as dioxygen pre-coverage, duration of the bombardment, and electron energy, this effect could be developed to a reproducible, clean, and safe method for producing chemisorbed oxygen suitable for further investigations. Up to 50 % of the initially physisorbed oxygen can be converted into chemisorbed oxygen, which desorbs above 500 K, following second-order kinetics (with a desorption energy of 140 ± 3 kJ/mol) at low coverages. A desorption order of two is indicative of the associative desorption, i.e., the adsorbate consists actually of oxygen *atoms* – a result that is confirmed by UP and NEXAFS spectra, both of which lack signals of occupied or unoccupied *di*oxygen molecular orbitals. At higher oxygen coverages ($0.35\ \text{ML} < \Theta < 1.0\ \text{ML}$), the desorption process is auto-inhibited, leading to a high-temperature shift combined with a reduced width of the thermal desorption peak. The sub-monolayer desorption spectra could be simulated on the basis of a kinetic model that includes formation of oxygen islands and desorption from a phase equilibrium between

two-dimensional condensed and gas phases. Alternatively, the spectra could also be described by a mechanism involving a strongly coverage-dependent desorption activation energy. Unfortunately there is no reasonable explanation for this coverage-dependence. Above monolayer coverage, another desorption peak emerges around 490 K; this peak is attributed to the decomposition of gold oxide. In addition to not forming an ordered adsorbate structure (a property common to all adsorbates investigated in this work), the chemisorbed oxygen also displaces the surface gold atoms of the substrate lattice as indicated by a complete suppression of the respective LEED reflexes. This rearrangement of the gold atoms by chemisorbed oxygen may reflect the directional and, thus, covalent contributions to the oxygen-gold bond.

The activation energy of dissociative chemisorption by far exceeds the desorption energy of chemisorbed oxygen. As a result, chemisorbed oxygen is a thermodynamically unstable, *endothermic* compound with a positive adsorption enthalpy of $\Delta H_{ad} \approx 190$ kJ per mol O_2 (see Fig. 12.1). Since adsorption entropies are generally negative, $\Delta S_{ad} < 0$, the adsorption Gibbs energy is also positive, $\Delta G_{ad} = \Delta H_{ad} - T\Delta S_{ad} > 0$. Thus, chemisorbed oxygen is also *endergonic*; its spontaneous formation is not only slow, it is thermodynamically forbidden.

Electron bombardment of physisorbed O_2 produces only chemisorbed oxygen species *on* the gold surface. In contrast, bombardment of the gold surface with O^+/O_2^+ ions leads to the additional occupation of bulk sites. Thermal desorption measurements performed subsequent to the ion bombardment (using ion energies between 1 keV and 5 keV) revealed four oxygen desorption states between 350 and 950 K which are associated with chemisorbed atomic oxygen ($E_{des} = 158$ kJ/mol), oxygen atoms dissolved in the bulk (204 kJ/mol), and gold oxide (103 kJ/mol). The relative TD signal intensities – and also the desorption temperatures – depend strongly on the ion energy and, hence, on the penetration depth of the ions. As expected, higher ion energies favour occupation of bulk sites, whereas lower energies promote formation of chemisorbed oxygen and surface gold oxide. The assignment of the bulk species was also confirmed by its inertness towards CO. The work function of the oxygen-sputtered surface has a complex temperature dependence. The on-surface oxygen species causes a suppression of the substrate LEED spots that is characteristic of oxygen chemisorption on gold, since this suppression was also found in the case of the species generated by electron-bombardment of physisorbed oxygen.

Moving further to the right in Fig. 12.1, we come to carbon monoxide adsorption. CO is weakly chemisorbed on gold. The isosteric heat of adsorption (which equals the CO-Au binding energy in the case of mobile adsorption) has an initial value of 59 kJ/mol and decreases rapidly with coverage, indicating substantial CO - CO repulsion, in agreement with TDS results. Below 150 K, CO adsorbs non-dissociatively with high initial sticking probability, $S_0 = 0.9$ at 28 K. Thermal desorption spectra show at least five desorption states between 32 K and 150 K corresponding to desorption energies between 8 and

38 kJ/mol. According to TDS, chemisorbed and physisorbed CO coexist in the first layer, a result that was corroborated by UV photoemission spectra. Results of angle-resolved UPS with polarized radiation suggests that the adsorbed CO molecules prefer an orientation parallel to the surface. CO adsorption has a complex influence on the surface potential and leads to a work function reduction of -0.95 eV at monolayer coverage. TDS and entropy measurements suggest that the state of chemisorbed CO at 160 K is best described by the model of a two-dimensional gas with partially frozen molecular rotation. No ordered CO overlayer structures were present over the whole coverage and temperature range. In the presence of a large defect concentration, e.g., after ion bombardment, an additional thermal desorption peak appears around 185 K; pre-adsorption of chemisorbed oxygen has a similar effect on the carbon monoxide TDS. Co-adsorption of carbon monoxide and krypton revealed that the most favourable adsorption sites for CO are less favourable for Kr, a result which reflects the different bonding mechanisms of CO (chemisorption) and Kr (physisorption). Thermal desorption spectra of CO and C_2H_4 agree in most features, suggesting a similar adsorbate-substrate bonding which is dominated by contributions from the Au (5d, 6sp) $\rightarrow \pi^*$ back-donation.

The reaction between pre-adsorbed atomic oxygen and CO molecules from the gas phase follows a Langmuir-Hinshelwood reaction and has a negative apparent activation energy of $\approx$ -2 kJ/mol. The activation energy of the reaction step CO(ad) + O(ad) $\rightarrow$ CO_2(ad) amounts to 57 kJ/mol, a value which exceeds the gas phase activation energy for this reaction (15 kJ/mol). The reactivity of chemisorbed oxygen reaches a maximum at 175 K in the presence of a CO pressure of 10^{-6} mbar. We found a CO/CO_2 conversion probability of 0.07 for this temperature and an oxygen coverage of 0.45 ML. Above 160 K, the total reaction rate decreases with increasing temperature. The most likely explanation is that an increasing temperature leads to a decrease of the CO coverage, an effect that is obviously not compensated by the simultaneous increase of the reaction rate constant. Compensation is not possible because the reaction activation energy is smaller than the CO desorption energy. The difference of both quantities is the apparent activation energy, which is negative. Since there is no reasonable explanation for the occurence of a negative activation energy without assuming that only adsorbed CO can react, our results strongly suggests the operation of a Langmuir-Hinshelwood mechanism. High initial oxygen coverages inhibit not only the thermal desorption, they inhibit the CO oxidation as well. This phenomenon is probably again connected with the formation of oxygen islands. As a consequence of this effect, the CO oxidation rate at any given time depends not only on the *instantaneous* oxygen coverage, but also on the *initial* oxygen coverage. Freshly prepared chemisorbed oxygen reacts with CO partially already at 45 K, well below the CO_2 desorption temperature of $\approx$ 100 K. This high reactivity indicates that oxygen species with a much lower activation energy for the CO oxidation exist initially. Heating to 450 K leads to a deactivation of these reactive species without oxygen desorption, and the resulting phase reacts with a uniform activation energy of 56 kJ/mol.

The reaction product carbon dioxide (CO_2) desorbs from the clean gold surface above 90 K with a desorption energy between 22 and 26 kJ/mol; pre-adsorption of oxygen leads to a higher binding energy. Masel [Ma96] pointed out that, on a good catalyst, the products usually possess binding energies of 5-20 kcal/mol (≈ 20-80 kJ/mol). Gold-based CO oxidation catalysts fall in this range, at least if the product CO_2 desorbs from gold. The CO_2 thermal desorption spectra exhibit strongly overlapping submonolayer and multilayer peaks, features that indicate that the intermolecular CO_2-CO_2 attraction is of similar strength as the CO_2-gold interaction. Thus, layer-by-layer growth and three-dimensional growth are equally favoured. Certain pecularities in the thermal desorption spectra such as simultaneous growth of a low-temperature and a high-temperature state and the second-layer peak appearing below the multilayer desorption temperature can be explained by three-dimensional growth. The relatively large surface enthalpy of small crystallites leads to a reduction of the desorption energy (Kelvin effect), whereas larger crystallites inhibit the desorption because they exclude a certain fraction of the total coverage from desorption. Pre-adsorption of oxygen increases the CO_2 desorption energy and leads to repulsive interactions in the first layer. This effect can most likely be attributed to the increased polarization of the molecules on the more polar oxidized surface. Successful (semi-)quantitative simulations of the thermal desorption spectra support our model of the CO_2 adsorbate structure on clean and oxidized gold.